Integration of rice apocarotenoid profile and expression pattern of Carotenoid Cleavage Dioxygenases reveals a positive effect of -ionone on mycorrhization

Plant Physiology and Biochemistry 207 (2024) 108366

Contents lists available at ScienceDirect

Plant Physiology and Biochemistry

journal homepage: www.elsevier.com/locate/plaphy

Integration of rice apocarotenoid profile and expression pattern of *Carotenoid Cleavage Dioxygenases* reveals a positive effect of β-ionone on mycorrhization

Cristina Votta [a,1], Jian You Wang [b,1], Nicola Cavallini [c], Francesco Savorani [c], Arianna Capparotto [d], Kit Xi Liew [b], Marco Giovannetti [a,d], Luisa Lanfranco [a], Salim Al-Babili [b,e,**], Valentina Fiorilli [a,*]

[a] Department of Life Sciences and Systems Biology, University of Torino, Viale Mattioli 25, Torino, 10125, Italy
[b] The BioActives Lab, Center for Desert Agriculture, King Abdullah University of Science and Technology, Thuwal, 23955-6900, Saudi Arabia
[c] Department of Applied Science and Technology (DISAT), Polytechnic of Turin, Corso Duca Degli Abruzzi 24, 10129, Torino, Italy
[d] Department of Biology, University of Padova, Via Ugo Bassi 58/b, 35131, Padova, Italy
[e] The Plant Science Program, Biological and Environmental Science and Engineering Division, King Abdullah University of Science and Technology, Thuwal, 23955-6900, Saudi Arabia

ARTICLE INFO

Keywords:
Apocarotenoids
Arbuscular mycorrhizal symbiosis
Carotenoid cleavage dioxygenases
Rice
Strigolactone
Zaxinone
β-ionone

ABSTRACT

Carotenoids are susceptible to degrading processes initiated by oxidative cleavage reactions mediated by *Carotenoid Cleavage Dioxygenases* that break their backbone, leading to products called apocarotenoids. These carotenoid-derived metabolites include the phytohormones abscisic acid and strigolactones, and different signaling molecules and growth regulators, which are utilized by plants to coordinate many aspects of their life. Several apocarotenoids have been recruited for the communication between plants and arbuscular mycorrhizal (AM) fungi and as regulators of the establishment of AM symbiosis. However, our knowledge on their biosynthetic pathways and the regulation of their pattern during AM symbiosis is still limited. In this study, we generated a qualitative and quantitative profile of apocarotenoids in roots and shoots of rice plants exposed to high/low phosphate concentrations, and upon AM symbiosis in a time course experiment covering different stages of growth and AM development. To get deeper insights in the biology of apocarotenoids during this plant-fungal symbiosis, we complemented the metabolic profiles by determining the expression pattern of *CCD* genes, taking advantage of chemometric tools. This analysis revealed the specific profiles of *CCD* genes and apocarotenoids across different stages of AM symbiosis and phosphate supply conditions, identifying novel reliable markers at both local and systemic levels and indicating a promoting role of β-ionone in AM symbiosis establishment.

1. Introduction

Carotenoids represent a widespread class of tetraterpene (C_{40}) lipophilic pigments synthesized by all photosynthetic organisms, including bacteria, algae, and plants, and by numerous non-photosynthetic microorganisms (Moise et al., 2014; Nisar et al., 2015). In plants, carotenoids are essential constituents of the photosynthetic apparatus where they act as photo-protective pigments and take part in the light-harvesting process. Further, these pigments have ecological functions, providing flowers and fruits with specific colors and flavors that attract insects and other animals or act as a repellent for pathogens and pests (Cazzonelli, 2011).

The carotenoid structure, rich in electrons and conjugated double bonds, makes them susceptible to oxidation, which causes the breakage of their backbone and leads to a wide range of metabolites called apocarotenoids (Moreno et al., 2021). These compounds can be

* Corresponding author.
** Corresponding author. The BioActives Lab, Center for Desert Agriculture, King Abdullah University of Science and Technology, Thuwal, 23955-6900, Saudi Arabia.
E-mail addresses: salim.babili@kaust.edu.sa (S. Al-Babili), valentina.fiorilli@unito.it (V. Fiorilli).
[1] These authors contributed equally to this work.

https://doi.org/10.1016/j.plaphy.2024.108366
Received 3 August 2023; Received in revised form 9 January 2024; Accepted 10 January 2024
Available online 11 January 2024

generated by non-enzymatic processes that are triggered by reactive oxygen species (ROS) (Harrison and Bugg, 2014; Ahrazem et al., 2016) or by the action of a ubiquitous family of non-heme iron enzymes, Carotenoid Cleavage Dioxygenases (CCDs) (Jia et al., 2018).

The genome of the model plant *Arabidopsis thaliana* encodes nine members of the CCD family, including five *NINE-CIS-EPOXY CAROTENOID CLEAVAGE DIOXYGENASES* (*NCED2, NCED3, NCED5, NCED6,* and *NCED9*) and four *CCDs* (*CCD1, CCD4, CCD7,* and *CCD8*) (Tan et al., 2003; Sui et al., 2013). In short, NCEDs catalyze the first step in abscisic acid (ABA, C_{15}) biosynthesis, *i.e.* the cleavage of 9-*cis*-violaxanthin or 9′-*cis*-neoxanthin into the ABA precursor xanthoxin (Nambara and Marion-Poll, 2005; Ahrazem et al., 2016). CCD1 cleaves several carotenoids and apocarotenoids at different positions along their hydrocarbon backbone (Schwartz et al., 2001; Vogel et al., 2008; Ilg et al., 2009, 2014; Jia et al., 2018) generating volatiles, such as β-ionone and geranylacetone, and a diverse set of dialdehydes in fruits and flowers of many plant species (Moreno et al., 2021). CCD4 enzymes are known to produce apocarotenoid-derived pigments, flavors, and aromas *in planta*, but their cleavage specificities differ considerably from those of CCD1 enzymes (Schwartz et al., 2001; Auldridge et al., 2006; Ilg et al., 2009; McQuinn et al., 2015; Hou et al., 2016). In plants, two different forms of CCD4 are present (Huang et al., 2009; Mi and Al-Babili, 2019): the first one is common in *Citrus* and is involved in forming the pigment citraurin (3-hydroxy- β-apo-8′-carotenal, C_{30}) formation by catalyzing a single cleavage reaction at the 7′,8′ double bond of zeaxanthin and β-cryptoxanthin (Ma et al., 2013; Rodrigo et al., 2013), while the other type cleaves bicyclic all-*trans*-carotenoids at the C9, C10 or C9′, C10′ double bond leading to apo-10′-carotenoids (C_{27}) and the corresponding C_{13} cyclohexenones, e.g. β-ionone (Bruno et al., 2015, 2016). Recently, a Gardinia CCD4 enzyme (GjCCD4a) was shown to catalyze sequential cleavage of β-carotene and zeaxanthin at the C7, C8 and C8′, C9′ leading to crocetin dialdehyde, the precursor of the saffron pigment crocin, and to cyclocitral and 3-hydroxy-cyclocitral, respectively (Zheng et al., 2022).

The two CCD-subfamilies CCD7 and CCD8 are involved in the biosynthesis of the plant hormone strigolactones (SLs) (Wang et al., 2021). CCD7 cleaves 9-*cis*-β-carotene (C_{40}), yielding β-ionone and 9-*cis*-β-apo-10′-carotenal (C_{27}); while CCD8 converts 9-*cis*--apo-10′-carotenal (C_{27}) *via* a combination of different reactions into the SL precursor carlactone (C_{19}) and ω–OH–(4-CH3) heptanal (C_8) (Alder et al., 2012; Chen et al., 2022). In addition, CCD7 may also catalyze the initial 9,10 cleavage required for mycorradicin synthesis (Floss et al., 2008).

A recent survey on plant genomes identified the *ZAXINONE SYNTHASE* (*ZAS*) as a representative for a further CCD subfamily, which is conserved in most land plants but missing in non-mycorrhizal species, i.e., *A. thaliana* (Fiorilli et al., 2019; Wang et al., 2019). *In vitro*, this enzyme cleaves the apocarotenoid 3-OH-β-apo-10′-carotenal (C_{27}) at the C13–C14 double bond, generating zaxinone, a C_{18}-ketone (3-OH-β-apo-13-carotenone) that acts as a growth regulator, and an unstable C_9-dialdehyde (Wang et al., 2019). Loss-of-function *zas* mutant showed a decreased zaxinone content in roots, reduced shoot and root growth, and a higher SL level compared to wild-type rice plants (Wang et al., 2019). Phylogenetic analyses revealed that the rice genome encodes three *OsZAS* homologs, named *OsZAS1b*, *OsZAS1c*, and *OsZAS2* (Ablazov et al., 2023). Intriguingly, although OsZAS2 is placed in a different clade from that of ZAS, it catalyzes the same reaction, and both enzymes contribute to zaxinone production in rice (Ablazov et al., 2023). Notably, ZAS homologues have also been named as CCD10 in *Zea mays* and *Nicotiana tabacum* (Zhong et al., 2020; Li et al., 2022), while, their catalytic functions, *e.g.* substrate specificity, are different from OsZAS in *in vitro* assays. However, the *in vivo* products and the biological functions of CCD10 need to be clarified.

Apocarotenoids play several roles in plants, from regulating root and shoot developmental processes to coordinating plant responses to abiotic and biotic stress (Moreno et al., 2021). They are also emerging signaling molecules implicated in plant-microbe interactions, including the arbuscular mycorrhizal (AM) symbiosis (Fiorilli et al., 2019). The AM symbiosis is one of the most ancient and widespread associations, formed by approximately 70% of land plants (Wang and Qiu, 2006; Brundrett, 2009), including major crops, with soil fungi belonging to the Glomeromycotina group (Spatafora et al., 2016). In this symbiosis, the fungus facilitates the plant uptake of minerals, predominantly phosphorus (P) and nitrogen (N) (Smith et al., 2011), and the tolerance to biotic and abiotic stress (Pozo et al., 2010; Chen et al., 2018). Meanwhile, the plant provides the fungus with fixed organic carbon. The establishment of the AM symbiosis includes several steps, starting with partner recognition *via* diffusible molecules that activate the common symbiosis signaling pathway (MacLean et al., 2017) and trigger the development of fungus adhesion structures, called hyphopodia, on the root epidermis. These structures permit the fungus to enter the host root tissues and proliferate within cells or intracellularly (Bonfante and Requena, 2011; Nadal and Paszkowski, 2013). Finally, fungal hyphae invade the inner cortical layers, penetrate single cells and form highly branched tree-shaped hyphal structures, the arbuscules, where nutrient exchanges occur (Harrison, 2012; Gutjahr and Parniske, 2013). During these stages, the plant controls fungal expansion and symbiotic functions, by activating a series of cellular, metabolic, and physiological changes (Gutjahr, 2014; Carbonnel and Gutjahr, 2014). Among the environmental factors that regulate AM colonization, phosphate (Pi) availability is certainly one of the most crucial ones (Smith et al., 2011; Richardson et al., 2011). It has been recently shown that a complex gene network centered on the plant Pi starvation response actively supervises AM fungal development in roots, acting at the local and systemic level (Shi et al., 2021; Das et al., 2022). Pi starvation also induces SL biosynthesis and release (Yoneyama et al., 2007; Wang et al., 2017, 2022), while high Pi levels repress the expression of genes involved in the biosynthesis of carotenoids and SLs in root (Carbonnel and Gutjahr, 2014; Haider et al., 2023), as well as the colonization by AM fungi (Breuillin et al., 2010; Balzergue et al., 2013). SLs are the best-known plant molecules active in the pre-symbiotic interaction with AM fungi. In Pi-starved plants, SLs are produced by roots and exported to the rhizosphere, which directly stimulates AM fungal metabolism, gene expression, and hyphal branching, supporting the development of this symbiosis Waters et al. (2017); Müller and Harrison (2019); Notably, Volpe et al., 2023 recently showed that SL biosynthesis is stimulated by chito-oligosaccharides released by AM fungi.

Studies of the last decade highlighted that other apocarotenoid compounds are involved in the AM symbiosis (Fiorilli et al., 2019 and reference therein), including the plant hormone ABA that is known for coordinating plant response to biotic and abiotic stress factors (Felemban et al., 2019; Moreno et al., 2021). ABA has been reported to be involved in mycorrhizal colonization in different host plants, probably through synergistic and antagonistic interactions with other hormones (Herrera-Medina et al., 2007; Martín-Rodríguez et al., 2011; Charpentier et al., 2014). Specifically, a positive correlation between ABA levels and SL biosynthesis was observed, suggesting that ABA and SLs collaborate to influence the outcome of the symbiosis (López-Ráez et al., 2010). In contrast, ABA controls the normal development of arbuscules by inhibiting ethylene production (Martín-Rodríguez et al., 2011) and acts as an antagonist of gibberellins (GA) by down-regulating their biosynthesis and promoting their catabolism (Floss et al., 2013; Martín-Rodríguez et al., 2016).

Blumenols (C_{13}) and mycorradicin (C_{14}) are further apocarotenoids clearly associated with AM symbiotic establishment and maintenance (Walter et al., 2007; Floβ et al., 2008; Floss et al., 2008; Fiorilli et al., 2019) and described as a signature for AM symbiosis since they are specifically accumulated in mycorrhizal plants (Walter et al., 2007; Hill et al., 2018; Moreno et al., 2021). Mycorradicins cause typical yellow/orange pigmentation of roots, which enabled their identification (Scannerini and Bonfante-Fasolo, 1977; Klingner et al., 1995; Floss et al., 2008). Blumenols are accumulated in roots and shoots of host plants in

direct correlation with the fungal colonization rate (Klingner et al., 1995; Maier et al., 1997; Walter et al., 2000; Fester et al., 2002; Strack and Fester, 2006). Even if their biological role has not yet been clarified, blumenols have been proposed as foliar markers that allow rapid detection of AM symbiosis and screening of functional AM associations (Walter et al., 2010; Wang et al., 2018). Finally, zaxinone, a recently discovered apocarotenoid growth regulator (Wang et al., 2019; Ablazov et al., 2020), is also involved in AM symbiosis and acts as a component of a regulatory network that includes SLs, as demonstrated by that the impact of the rice gene encoding *Zaxinone Synthase* (*OsZAS*) on the extent of AM colonization SLs (Votta et al., 2022). Albeit the significant progress that has been recently made in the field of plant apocarotenoids, our knowledge on the regulation of their biosynthesis by phosphate homeostasis, plant developmental and AM symbiosis stages in different organs is still limited.

In the current study, we set out to further explore the involvement of apocarotenoids in the AM symbiosis and to identify novel local and systemic AM markers. For this purpose, we generated a qualitative and quantitative profile of apocarotenoids in roots and shoots of rice plants exposed to high/low Pi concentrations (+Pi and -Pi) and upon AM symbiosis in a time course experiment covering different stages of growth and AM development. We complemented the metabolic profiles by characterizing the expression pattern of *CCD* genes and took advantage of chemometric tools to get deeper insights into the biology of apocarotenoids during this plant-fungal symbiosis. To validate our datasets, we treated mycorrhizal plants with β-ionone (Apo9), identified as an AM-induced compound. Our results demonstrate for the first time that β-ionone supply increases AM fungal colonization in rice, pointing to its involvement in AM symbiosis and highlighting the robustness of our database.

2. Materials and methods

2.1. Plant and fungal materials

Wild type rice seeds (cv. Nipponbare) were germinated in pots containing sand and incubated for 10 days in a growth chamber under 14 h light (23 °C)/10 h dark (21 °C). A set of plants (MYC) was inoculated with *Funneliformis mosseae* (BEG 12, MycAgroLab, France). The fungal inoculum composed of propagules and sporocarps (15%) was mixed with sterile quartz sand and used for colonization. A group of non-mycorrhizal plants (no-myc -Pi) was also set up using only sterile quartz send as substrate. These two sets of plants (MYC and no-myc -Pi) were grown in 12-cm-high and 10-cm-diameter pots (1.2 dm^3) watered with 40 mL a modified Long-Ashton (LA) solution containing 3.2 μM $Na_2HPO_4{\cdot}12H_2O$ (low Pi) (Hewitt, 1966) and grown in a growth chamber under 14 h light (24 °C)/10 h dark (20 °C) regime. Another set of no-myc plants was watered with 40 mL of a LA containing 500 μM $Na_2HPO_4{\cdot}12H_2O$ (+Pi) and grown in the same condition described above; these plants represented the no-myc + Pi samples. Plants for the three different conditions (MYC, no-myc -Pi, no-myc + Pi) were collected at three time points: 7 days post-inoculation (dpi), 21 dpi, and 35 dpi. For the molecular (gene expression level), physiological (phosphate content) and metabolites (apocarotenoid quantification) analyses, roots and shoots samples were harvested and immediately frozen in liquid nitrogen and stored at −80 °C. Roots and shoots samples of a set of plants for each condition were lyophilized to determine the dry weight and to quantify the phosphate concentration level in the shoots. For all the time points, mycorrhizal roots were stained with cotton blue, and the level of mycorrhizal colonization was assessed according to Trouvelot et al. (1986) using MYCOCALC (http://www2.dijon.inra.fr/mychintec/Mycocalc-prg/download.html).

To evaluate the impact of β-ionone on AM fungal colonization in rice, seeds of rice plants (cv. Nipponbare) were germinated and inoculated with *F. mosseae* as described before. Plants were watered with a low Pi Long-Ashton (LA) solution. A set of WT plants were treated with 50 nM β-ionone, by applying the molecule once a week directly in the nutrient solution. AM colonization was evaluated by means of molecular (*OsPT11* and *OsLysM* gene expression level) and morphological (Trouvelot et al., 1986) assays at 35 dpi. In parallel, to assess the impact of β-ionone supply on SLs biosynthesis, a set of non-mycorrhizal and mycorrhizal plants were treated or not with 50 nM β-ionone. By means of molecular approach (*CCD8* gene expression level) we evaluated the impact of β-ionone on SLs biosynthesis in treated and non-treated non-myc and MYC plants. The experiments were repeated twice.

2.2. Inorganic phosphate concentration measurements

Samples of rice leaves were collected, freeze-dried then weighed before being ground into powder using liquid nitrogen. The resulting powder was subjected to incubation at 98 °C in NanoPure water for 1 h, followed by centrifugation at maximum speed for 20 min. Next, a 1:10 dilution of the supernatant was prepared, and 25 μL of this dilution was used for measuring inorganic phosphate concentrations with a phosphate assay kit (Sigma #MAK308), following the instruction manual. Specifically, 50 μL of reagents were added to the samples, which were then kept in darkness for 30 min. Subsequently, the absorbance at 620 nm (OD 620) was measured using a spectrophotometer.

2.3. Qualitative and quantitative profiling of plant apocarotenoids (APOs)

Following the method used by Mi et al. (2018), about 20 mg lyophilized root and shoot tissue powder was spiked with Internal Standards (IS) mixture (2 ng each standard) and extracted with 2 mL of methanol containing 0.1% butylated hydroxytoluene (BHT) in an ultrasound bath (Branson 3510 ultrasonic bath) for 15 min, followed by the centrifugation. The supernatant was collected, and the pellet was re-extracted with 2 mL of the same solvent. The two supernatants were then combined and dried under vacuum. The residue was re-dissolved in 150 μL of acetonitrile and filtered through a 0.22 mm filter for LC-MS analysis.

Analysis of apocarotenoids was performed on a Dionex Ultimate 3000 UHPLC system coupled with a Q-Orbitrap-MS (Q-Exactive plus MS, Thermo Scientific) with a heated electrospray ionization source. Chromatographic separation was carried out on an ACQUITY UPLC BEH C_{18} column (100 × 2.1 mm, 1.7 μm) with a UPLC BEH C18 guard column (5 × 2.1 mm, 1.7 mm) maintained at 35 °C. UHPLC conditions including mobile phases and gradients were optimized based on the separation of APOs and the time needed for sample analysis. APO isomers were identified by MS/MS fragmentation.

The quantification of APOs was calculated as follows: Amount [target APO] = Area [target APO]/Area [spiked IS] x Amount [spiked IS]/mg materials. The apocarotenoid profiles were determined twice, using the same experimental set-up and analyzing two independent sets of plants.

2.4. Gene expression analysis

Total RNA was extracted from WT rice roots using the Qiagen Plant RNeasy Kit according to the manufacturer's instructions (Qiagen, Hilden; Germany). Following the producer's directives, samples were treated with TURBO™ DNase (Thermofischer). The RNA samples were routinely checked for DNA contamination through PCR analysis. Single-strand cDNA was synthesized from 1 μg of total RNA using Super-Script II (Invitrogen) according to the instructions in the user manual. Quantitative RT-PCR (qRT-PCR) was performed using a Rotor-Gene Q 5plex HRM Platform (Qiagen). All reactions were performed on at least three biological and three technical replicates. Baseline range and take-off values were automatically calculated using Rotor-Gene Q 5plex software. The transcript level of genes listed in Table S1 was normalized using two housekeeping genes (*OsRubQ1* and *OsActin*) (Güimil et al.,

2005). Only take-off values leading to a Ct mean with a standard deviation below 0.5 were considered.

2.5. Statistics and reproducibility

Both experiments (plant apocarotenoid quantification and CCD gene expression analysis) were performed twice considering each experiment at least three biological replicates. Statistical tests were carried out through One-way Analysis of Variance (One-way ANOVA) and Tukey's *post hoc* test, using a probability level of $P < 0.05$. All statistical elaborations were performed using PAST statistical package version 4 (Hammer et al., 2001).

2.6. Data quality assessment and preprocessing

Gene and apocarotenoid datasets were inspected to spot potential extreme samples or outliers. Different preprocessing approaches were tested, including autoscaling (i.e., column scaling to unit variance, followed by mean centering) and normalization to a unit area (i.e., the normalization factor of each sample was computed from its "area under the curve") followed by mean centering. Based on the ease of interpretation, we selected the following preprocessing: mean centering alone for the apocarotenoids dataset, and autoscale for the gene expression dataset. All modeling results were therefore obtained from the two datasets preprocessed as such. With respect to the analysis with the low-level data fusion approach (i.e., combining the two datasets into an individual one), a different sequence tailored to the issue of obtaining an equal representation of the two datasets was used, as described in the dedicated paragraph further in the section Data fusion approach.

2.7. Exploratory analysis

All chemometric models reported in this work are "exploratory", meaning that they describe the phenomena and natural groupings captured in the data, in an unsupervised manner (Li Vigni et al., 2013). To this aim, Principal Component Analysis (PCA) (Bro & K. Smilde, 2014) was employed. This technique is employed to capture, in sequence, the largest sources of variability by defining new variables (the so-called "Principal Components", PCs), which are summaries of the different pieces of information contained in the data. This "summarized" version of the information can be inspected with the scores and loadings plots, which are scatter plots obtained by plotting pairs (and sometimes triplets) of PCs. The scores plot allows inspecting the relationships among the samples and thus spotting possible groupings and tendencies or patterns of interest, while the loadings plot allows inspecting the relationships among the variables of the data, providing at the same time an interpretation of the scores plot. In our study, individual apocarotenoids and genes were identified by their systematic names and inspected in PCA as the samples. At the same time, the variables of the datasets were the combinations of three-time points (7, 21, and 35 dpi) and three conditions (MYC, no-myc -Pi, no-myc + Pi) for a total of nine combinations.

2.8. Data fusion approach

For this study, we also tested a low-level data fusion approach (Borràs et al. 2015) to combine and jointly explore the information of the apocarotenoids and genes datasets. In practice, the apocarotenoids dataset was joined with the genes dataset in the sample direction so that the nine variables (combinations of time points and conditions) were coherent between the two datasets, i.e., the information described by each column had to be the same in both datasets.

We performed the following data preprocessing and fusion sequence: (i) standard deviation scaling for each APO/gene quantification, (ii) fusion of the two data tables, (iii) group scale to give the two data tables the same importance (i.e., each dataset accounts for 50 % of the total variance of the resulting fused dataset), (iv) mean center. The new fused data table was then modelled with PCA, with the apocarotenoids and the genes as the samples (rows) and the combinations of time points and treatments as the variables (columns) (Fig. S1).

3. Results

3.1. Plant biomass, Pi content and mycorrhizal colonization assessment

To assess the impact of Pi availability on plant biomass at different time points during mycorrhization, we individually collected and lyophilized shoots and roots from plants grown at low (3.2 μM) and high (500 μM) Pi and from MYC plants grown at low Pi. Roots and shoots biomass was quantified by measuring the dry weight (DW). No statistical differences were detected among treatments at the different time points, neither in roots nor in shoots (Figs. S2A and B). Moreover, to determine if the low/high Pi supply and the mycorrhizal condition influenced Pi content, we quantified the Pi concentration in the shoots during the different stages (Fig. S2 C). As expected, the plants grown under high Pi level displayed higher Pi content in the shoots at all time points considered. The Pi content of shoots of MYC plants was lower at the early stage (7 dpi), compared to non MYC plants grown under high and low Pi, probably due to the Pi sequestration exerted by the AM fungus, while statistically higher Pi concentration was detected in the late stage (35 dpi) compared to non-mycorrhizal low Pi condition.

To monitor the AM symbiosis development, we measured the transcript levels of plant AM marker genes (*OsPT11* and *OsLyM*) and AM fungal housekeeping (*Fm18*) at the early (7 dpi), middle (21 dpi), and late (35 dpi) stage (Fig. S3A). The expression of all the tested genes increased over the time. In agreement with the molecular results, the morphological analysis performed by Trouvelot method confirmed that root colonization (F% and M%) and the arbuscules abundance (A% and a%) increased over time (Fig. S3B).

3.2. CCD gene expression pattern during AM symbiosis

We determined the transcript level of a set of *CCD* genes, including *CCD1, CCD4a, CCD4b, CCD7, CCD8, ZAS1, ZAS1b, ZAS1c,* and *ZAS2*, in mycorrhizal plants grown at low Pi (3.2 μM) and in non-mycorrhizal plants grown at low (3.2 μM) or high Pi (500 μM). To assess the statistically significant differences, all samples were referred to the -Pi condition within each time point. As shown in the heatmap (Fig. 1A; S4A) referred to roots, *CCD1* and *CCD4b* transcript levels increased at 21 dpi in the +Pi condition compared to -Pi and MYC ones. Concerning the SL biosynthetic genes, we observed an induction of *CCD7* in MYC roots at the middle and late stage (21, 35 dpi), while *CCD8* was induced at 7 and 21 dpi under the MYC condition, and, as expected, down-regulated under + Pi condition in the later time points (at 21 and 35 dpi) (López-Ráez et al., 2008; Yoneyama et al., 2013). At the early and middle stage (7 and 21dpi), *ZAS1* showed an up-regulation in MYC samples and a down-regulation at 21 dpi under + Pi. The *ZAS1* homolog, *ZAS1b* was upregulated at 21 dpi in MYC, while we detected a down-regulation in MYC roots during the later stage. By contrast, *ZAS1c* was up-regulated at 21 and 35 dpi in MYC roots. Finally, *ZAS2* transcript level increased and decreased at 7 and 35 dpi in +Pi condition, respectively.

CCDs gene expression pattern in shoots (Fig. 1B, Fig. S4B) displayed several differences compared to roots. We detected lower *CCD1* expression level at 21 and 35 dpi in MYC and +Pi conditions. Under mycorrhizal condition, *CCD4a* showed an expression profile similar to that of *CCD1*, while it was also induced at 21 dpi at + Pi condition. By contrast, *CCD4b* displayed an opposite trend, compared to *CCD4a,* with an up-regulation at 35 dpi under the MYC condition. We observed significant down-regulation of *CCD7* (MYC and +Pi) and *CCD8* (+Pi) at 21 dpi that was maintained for both genes at 35 dpi in shoot of MYC plants. *ZAS1* displayed a down-regulation trend in all time points and

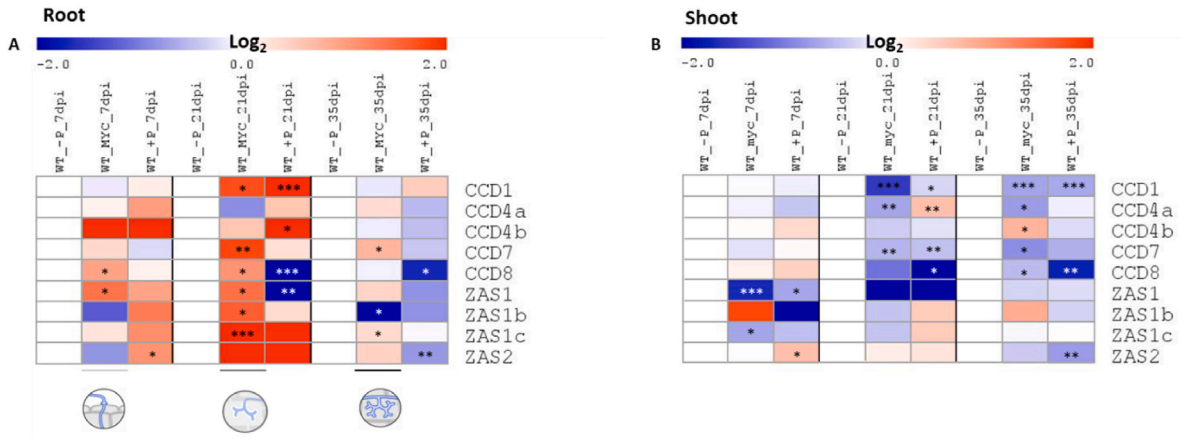

Fig. 1. Heatmap of root (A) and shoot (B) gene expression of the three time points (7, 21, 35 dpi: days post inoculation) and the three analyzed conditions (-Pi, myc, +Pi). Data are means ($n \geq 3$). For each gene and time point, the value of the corresponding -Pi sample was set to 1. Asterisks indicate statistically significant differences referred to the –Pi condition, separately for each time point, by one way-Anova (*$P < 0.05$; **$P < 0.01$; ***$P < 0.001$). The circles represented the different stages of mycorrhization: at the early stage (7 dpi), the fungus structures, hyphopodia, adhered to the root epidermis, during the middle stage (21 dpi), the arbuscules started their development that will be completed at the later stage (35 dpi). Heatmaps were generated with the MultiExperiment Viewer (MeV) software. -Pi: 3.2 μM Pi; myc: mycorrhizal plants grown at 3.2 μM Pi; +Pi:500 μM Pi.

conditions considered, with a statistically significant difference in mycorrhizal and +Pi samples at 7 dpi. We did not detect significant changes in *ZAS1b* expression level, while *ZAS1c* showed a down-regulation in leaves of the MYC plant at the first time point (7 dpi). Lastly, *ZAS2* was barely detected in the shoot of plant growth at low Pi, while it showed an up-regulation at 7 dpi under + Pi conditions and a down-regulation in +Pi at 35 dpi.

We used PCA to assess the samples' natural grouping and clustering tendencies under the different growth conditions (MYC, -Pi, and +P) at the three time points analyzed. The loadings plot of Fig. 2A describes the influence of the measured variables on the samples' distribution shown in the scores plot of Fig. 2B that provides insights into this distribution.

In our study, the PCA model was obtained from the expression level of the set of genes analyzed in all samples, in which PC1 explained 54.24% (related to the gene expression level) and PC2 explained 16.99% (related to the plant developmental stage) of the total variance (Fig. S5). The information described by PC1 and PC2 highlights that in all growth conditions the middle developmental stage (21 dpi) presented a different *CCD* expression pattern compared to early and late stages. We selected the model with 4 PCs, since PC3 (6.02%) and PC4 (11.21%) provided notable information related to the growth conditions, as shown in the loadings plot (Fig. 2A), while the scores plot (Fig. 2B) displayed a clear separation between the plant organs: roots and shoots. More in detail, Fig. 2B showed that *CCD8*, *ZAS1* and *CCD7* expression in roots was influenced by MYC condition while *CCD4a, CCD4b* and *CCD1,* expression was more affected by high Pi level. Concerning the shoot, *CCD1, CCD4a, CCD7, CCD8,* and *ZAS1* were located in the plot area influenced by the low Pi level.

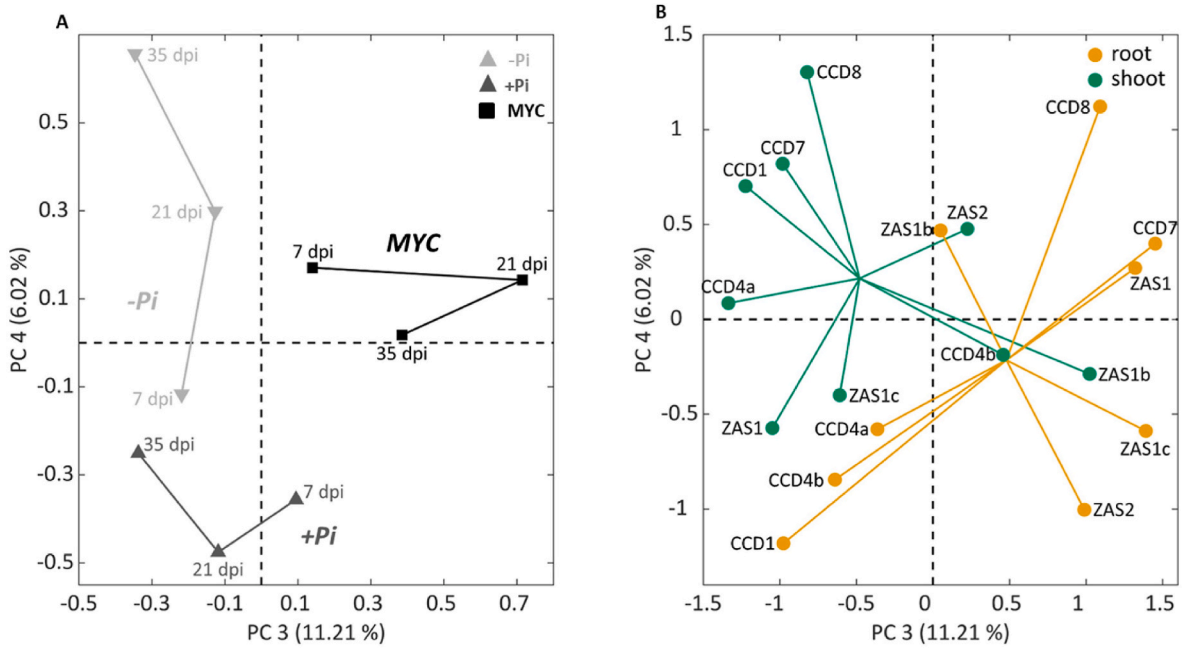

Fig. 2. Principal component analysis of root and shoot CCDs genes expression across the three time points and the three growth conditions (-P, myc, + P). Loadings plot (A) and scores plot (B) showing the third and fifth principal components. In the scores plot (B) for both groups the lines connecting each sample lead to the cluster center.

3.3. Apocarotenoid profile

To profile non-hydroxylated and hydroxylated apocarotenoids (Table S2) in roots and shoots of rice plants grown in high/low Pi concentration (+Pi and -Pi) and upon MYC condition, we used the ultra-HPLC (UHPLC)-mass spectrometry (MS)-based approach to get insight into the apocarotenoid compositions (Mi et al., 2018). To simplify this analysis, the statistically significant differences were referred to as the -Pi condition within each time point. The results showed a substantial difference between roots and shoots in the apocarotenoid quantification and distribution, in analogy to what has been observed in *CCDs* gene expression data.

With respect to roots (Fig. 3A, Fig. S6A), we observed an increment of the content of Apo9 (β-ionone), Apo10, and their hydroxylated forms (OH-Apo9 and OH-Apo10) in MYC condition at 21 dpi and 35 dpi. In addition, Apo10 showed a higher accumulation in MYC roots and upon + Pi at 7 dpi. Likewise, at the same time point, the Apo11 level increased in the MYC condition, while it decreased during the middle stage (21 dpi), contrary to its hydroxylated forms (OH-Apo 11 and OH-Apo 11-iso) that showed a strong accumulation. Moreover, at 35 dpi, all the β-apo-11-carotenoids (C_{15}) showed a statistically significant decrease upon + Pi. Apo12 and Apo14 displayed the same pattern at 35 dpi: both showed a higher accumulation in MYC and +Pi compared to -Pi. By contrast, we observed an increase of Apo13 in MYC and +Pi conditions during the early (7 dpi) and middle stages (21 dpi); its hydroxylated forms (OH-Apo13 and OH-Apo13-iso) also displayed a higher content at 7 dpi in the +Pi condition and 21 dpi in the MYC root. Moreover, at the later stage (35 dpi), OH-Apo13-iso showed a statistically significant higher and lower content in MYC and +Pi roots respectively. Finally, Apo15 and Apo15-iso displayed a higher level at 21 dpi in MYC and +Pi roots. Concerning the shoot, the heatmap (Fig. 3B) showed that the non-hydroxylated apocarotenoids (from Apo 8 to Apo 15) displayed an overall similar profile: a general decrease at 7 and 35 dpi in +Pi condition compared to plants grown at -Pi, and an increase upon MYC and +Pi during the middle stage (21 dpi). Notably, the levels of Apo9, Apo10, Apo12, Apo13, Apo14 and its isomer (Apo14-iso), decreased at 7 dpi in the +Pi condition. By contrast, at 21 dpi, Apo9, Apo10, Apo11, Apo12, Apo13, and Apo15 content increased in MYC and +Pi conditions, while Apo14 and its isomer showed an increment only for the MYC condition. At the later time point (35 dpi), we detected a decrease of Apo9, Apo12, and Apo14 and its isomer content in MYC plants.

The hydroxylated forms showed a profile similar to non-hydroxylated APO with an increased content at 21 dpi in the +Pi condition, and a decreasing trend in the MYC condition at 35 dpi. In detail, at 7 dpi, the OH-Apo11 isomer showed a statistically different increase in MYC condition. Further, at 21 dpi, OH-Apo8, OH-Apo10, OH-Apo11 and its isomer, OH-Apo12, OH-Apo13, OH-Apo15, and OH-Apo15 isomer strongly increase in +Pi. At the same time point, also OH-Apo11 isomer and OH-Apo13 levels increased in the MYC condition, while the OH-Apo10 content decreased. At the later stage, OH-Apo10 and OH-Apo11 displayed an increased content at +Pi, while OH-Apo13-iso accumulation decreased in the shoot of plants grown in MYC and +Pi conditions (Fig. S6B).

To highlight correlations in apocarotenoids distribution across different stages of plant development, AM symbiosis and Pi levels, a PCA was employed. In the apocarotenoid database, no outliers (i.e., samples with clearly inconsistent values and/or unexpected behaviors attributable to errors of measurement or to data acquisition problems) were identified, even if three apocarotenoids (OH-Apo10, Apo10, and Apo12) showed very high values across all time points and treatments (Fig. S7). To better model the information of the rest of the samples, these three extreme samples were removed from the apocarotenoid dataset and projected at a later stage to inspect their position in the final PCA model.

In the PCA model referred to apocarotenoids, PC1 explained 43.88% (related to apocarotenoid quantification) and PC2 explained 22.23% (related to growth conditions) of the total variance (Fig. S8). PC1 and PC2 models highlighted the apocarotenoids strictly related to MYC condition (OH-Apo9; Apo11; OH-Apo11; OH-Apo13iso). Further, we adopted the PCA model PC2 combined with PC3, where PC3 explained 2.55% of the total variation, upon the propensity of samples to regroup following the temporal trend described in the loadings plot (Fig. 4A).

In the plot chart, at 7 dpi all the growth conditions were clustered in the same area. Here, the majority of the analyzed shoot apocarotenoids (Apo9, Apo11, OH-Apo11 isomer, OH-Apo13, OH-Apo13 isomer, and Apo15) were located, suggesting that their content was mainly influenced by the growth time than by the growth condition.

The scores plot (Fig. 4B) displayed a clear separation between the apocarotenoids quantified in roots or shoots. In-depth, in root OH-Apo9, OH-Apo11, Apo11, and OH-Apo13 isomer were mainly influenced by mycorrhization in different time points (21 dpi and 35 dpi). Instead, APO14 seems to be dependent on the Pi level and MYC condition. However, in shoot OH-Apo9, OH-Apo12, and OH-Apo15 were linked to

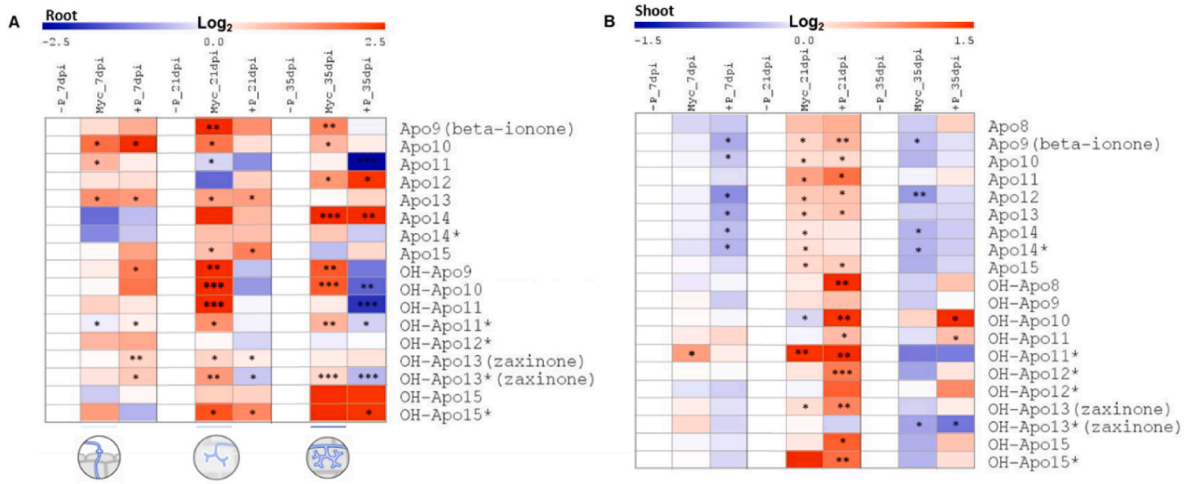

Fig. 3. Heatmap of root (A) and shoot (B) apocarotenoids quantification across the three time points and the three analyzed conditions (-P, MYC, + P). For each APOs and time point, the value of the corresponding -Pi was set to 1. Data are means ($n \geq 3$). Asterisks indicate statistically significant differences as compared to –P condition, separately for each time point, by one way-Anova (*P < 0.05; **P < 0.01; ***P < 0.001). The circles represented the different stages of mycorrhization: at the early stage (7 dpi), the fungus structures, called hyphopodia, adhered to the root epidermis, during the middle stage (21 dpi), the arbuscules started their development that will be completed at the later stage (35 dpi). The apocarotenoids indicated with asterisks represented the isoform of the corresponding apocarotenoid. Heatmaps were generated with the MultiExperiment Viewer (MeV) software. The experiment was performed twice reproducing comparable results.

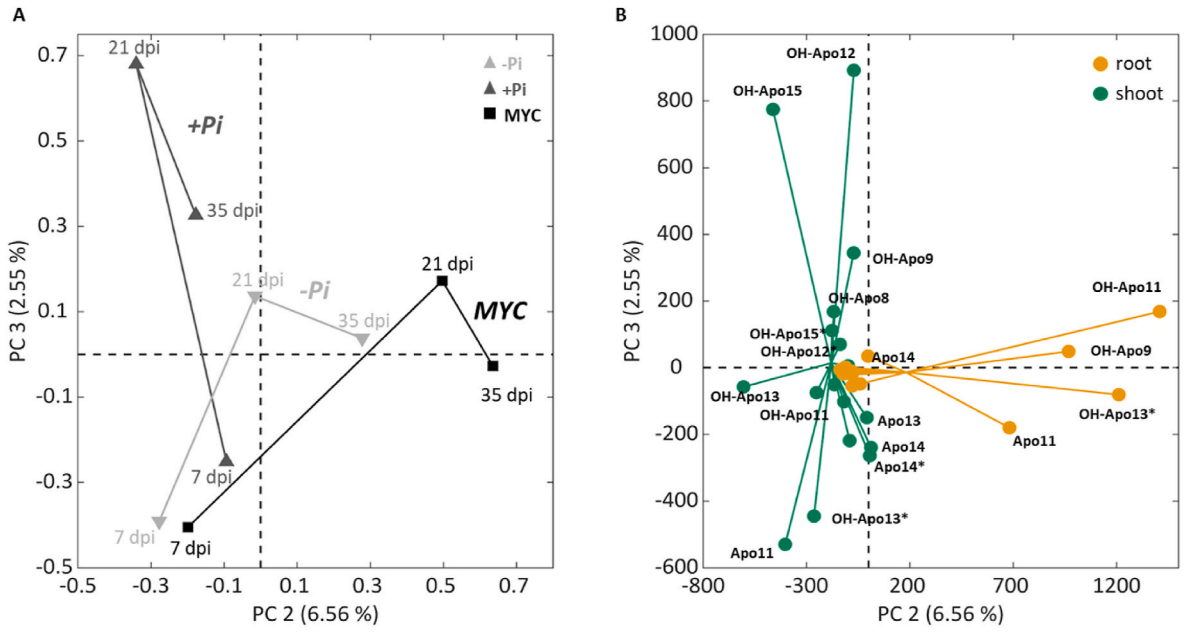

Fig. 4. Principal component analysis of root and shoot APOs across the three-time points and the three growth conditions (-Pi, MYC, + Pi). Loadings plot (A) and scores plot (B) show the second and third principal components. In the scores plot (B) for both groups the lines connecting each sample lead to the cluster center.

the +Pi condition. OH-Apo8, the OH-Apo12 isomer, and the OH-Apo15 isomer depended on the Pi level at the middle stage (21 dpi).

3.4. Data fusion

Finally, to combine and investigate the potential correlation between apocarotenoids and CCD genes, we used a low-level data fusion approach (Borràs et al., 2015) to combine the two datasets into an individual fused one, also modelled with PCA.

In the resulting PCA model, considering genes expression and apocarotenoids profiles joined, PC1 explained 30.23% and PC2 explained 27.21% of the total variance (Fig. 5A and B). From the loadings plot (Fig. 5A) we observed the grouping of the samples interpretable by the temporal trend (7, 21, and 35 dpi). As reported for the previous scores plots referred to individual categories (genes and apocarotenoids), in Fig. 5B we observed a clear separation between plant organs. In more detail, genes and apocarotenoids in the left bottom part of the scores plot (Fig. 5B) were more related to the early stage (7 dpi). Here, we found mainly shoot apocarotenoids, *CCD8* and *CCD7* expressed in shoot, and *ZAS1c* in the root. By contrast, the lower right part of the

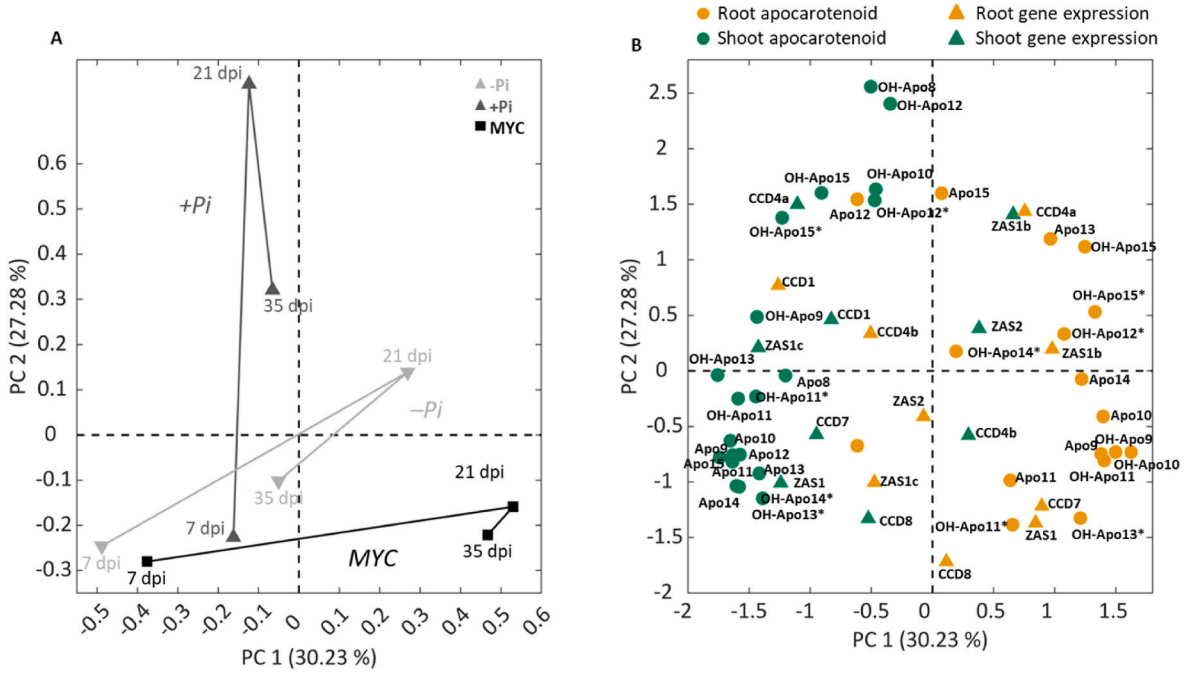

Fig. 5. Principal component analysis of root and shoot genes and apocarotenoids datasets fused and analyzed across the three-time points and the three growth conditions (-Pi, MYC, + Pi). Loadings plot (A) and scores plot (B) show the first and second principal components. The apocarotenoids indicated with asterisks represent the isoform of the corresponding apocarotenoid.

plot, clustered exclusively apocarotenoids and genes (*CCD7, CCD8* and *ZAS1*) modulated in the root, depended on the MYC condition. In particular, Apo9 (β-ionone), Apo10, and their hydroxylated forms (OH-Apo9 and OH-Apo10) were grouped in this plot area, suggesting their possible involvement during the AM colonization process. Furthermore, in the same area, we highlighted the association between *CCD7* and one of its cleavage products, Apo9 (β-ionone). In addition, this group highlighted the correlation between *ZAS1*, responsible for the OH-Apo13 (zaxinone and/or its isomer) synthesis, and its precursors (OH-Apo10) (Fig. S9). Interestingly, we also identified Apo11, OH-Apo11, and OH-Apo11-iso in this area.

In shoots, most of the *CCD* genes (*CCD1, CCD4a, CCD7, CCD8*, *ZAS1* and *ZAS2*) were mainly influenced by the Pi level. Moreover, the left area of the plot clustered the majority of shoot apocarotenoids. Generally, apocarotenoids profiles in the shoot seem to be more influenced by the time points (7, 21, 35 dpi) and Pi availability, whereas, in the root, most apocarotenoids and genes were mainly influenced by mycorrhization.

3.5. *β-ionone exogenous treatment with β-ionone increased AM colonization*

Considering that Apo 9 (β-ionone) was strongly accumulated in roots during the middle and later stages of AM symbiosis and that the genes (*CCD1* and *CCD7*) mediating its biosynthesis (Fig. S9) were induced in mycorrhizal roots (Fig. 1A; Fig. S4A; Fig. 3A; Fig. S6A), we evaluated the impact of this apocarotenoid on the establishment of the AM symbiosis. To test if β-ionone is involved in regulating this process, we assessed the AM colonization level in a set of mycorrhizal plants treated with β-ionone (50 nM) by morphological and molecular analysis. We observed that β-ionone treated plants showed higher percentage of frequency of mycorrhizal colonization (F%) and arbuscule abundance (a%) compared to untreated plants (Fig. 6A). Consistent with the morphological data, a significant increase of the expression of *OsPT11* and *OsLysM,* two rice AM marker genes (Fiorilli et al., 2015), in mycorrhizal root samples treated with the β-ionone, compared to the untreated mycorrhizal plants was detected (Fig. 6B and C). These results suggest that exogenous application of β-ionone promotes AM symbiosis and indicate its involvement in the symbiotic process. Moreover, these findings provide evidence for the reliability of our datasets. Since Felemban et al. (2023) demonstrated in Arabidopsis plants that exogenous treatment of β-ionone (5 μM) increments the *CCD8* and *CCD7* genes expression, we investigated whether the promoting role of β-ionone in AM symbiosis could be mediated by the alteration of SLs biosynthesis. We therefore evaluated the transcript level of *CCD8*, the SLs biosynthesis marker gene, in mycorrhizal and non-mycorrhizal conditions treated or not with 50 nM β-ionone. Neither in non-mycorrhizal nor in mycorrhizal roots we observed a statistically significant difference of *CCD8* gene expression upon β-ionone treatment (Fig. 6D). These results suggest that, at least at this concentration (50 nM), β-ionone influences AM symbiosis in a SL-independent manner.

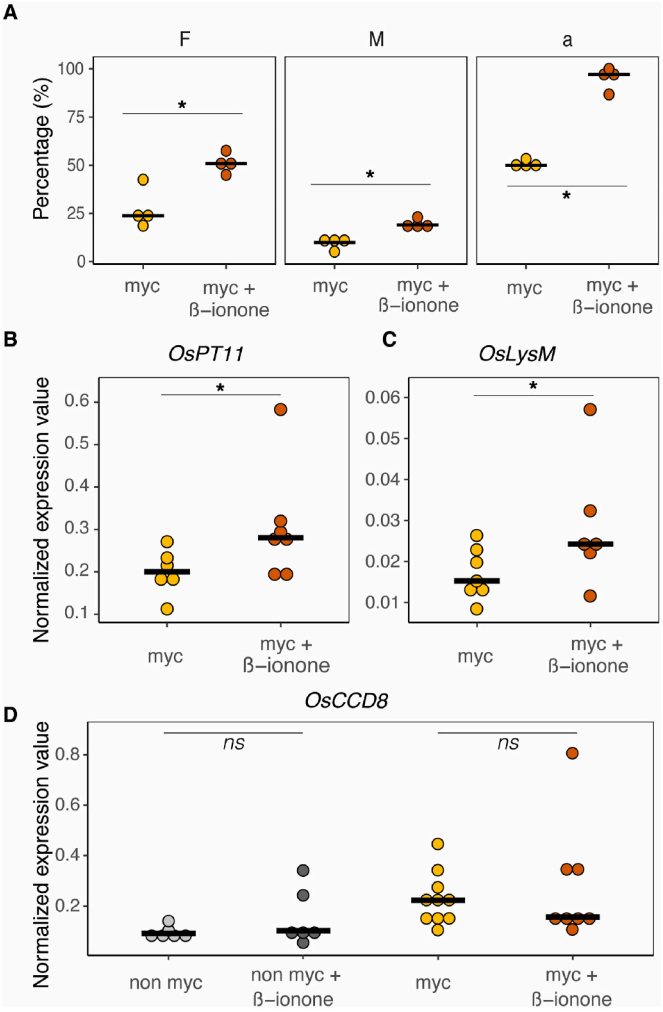

Fig. 6. Evaluation of β-ionone effects on the AM symbiosis and SLs biosynthesis gene expression. (A) Mycorrhizal colonization in non-treated and treated plants by the AM fungi *Funneliformis mosseae* at 35 dpi. Degree of colonization expressed as mycorrhizal frequency (F %), intensity (M %) and arbuscule abundance (a %) in the root system of rice plants non treated and treated with 50 nM β-ionone. Individual data for each condition are shown as dots and the median as black bars. (B,C) Molecular evaluation of mycorrhization by qRT-PCR analysis of mRNA abundance of plant AM-responsive genes (*OsPT11*, *OsLysM*) on mycorrhizal roots treated with 50 nM β-ionone (β-ionone) or non-treated. Individual data for each condition are shown as dots and the median as black bars. (D) Molecular evaluation of mycorrhization by qRT-PCR analysis of mRNA abundance of *CCD8* gene on non-mycorrhizal and mycorrhizal roots treated with 50 nM β-ionone (β-ionone) or non-treated. Individual data for each condition are shown as dots and the median as black bars. Statistical analysis was performed using one-way analysis of variance (ANOVA) and Tukey's post hoc test (*P < 0.05).

4. Discussion

In recent years, plant apocarotenoids are emerging not only as carotenoid breakdown products but as metabolites with active roles in regulating physiological and developmental processes and plant-(a)biotic interactions (Zheng et al., 2021). In particular, some apocarotenoids were associated with the establishment and maintenance of AM symbiosis (Fiorilli et al., 2019). Investigations over the last decades indicate that beyond SLs, ABA, mycorradicins, and blumenols (Walter et al., 2007; Floss et al., 2008; Hill et al., 2018; Wang et al., 2018; Fiorilli et al., 2019), other apocarotenoids may play a role in this mutualistic association. For example, zaxinone, generated by the activity of the CCD subfamily Zaxinone Synthases, was shown to control the extent of AM root colonization with a complex interplay with SLs (Votta et al., 2022; Ablazov et al., 2023). To further explore the involvement of other apocarotenoids during the AM symbiosis in this work we developed a combined approach: we profiled apocarotenoids in rice roots and shoots across a time course (7, 21, and 35 dpi) experiment of AM colonization by LC-MS (Mi et al., 2018) and, in parallel, we monitored the expression pattern of a set of *CCD* genes. To highlight genes and apocarotenoids more specifically related to the AM association, we analyzed plants grown in low and high Pi conditions. Our results show that the AM colonization, although confined to the root system, can trigger a systemic response which is evident from the modulation of *CCDs* gene expression and apocarotenoid content in rice shoots. The effect on epigeous organs exerted by AM root colonization has been already described in other species (Fiorilli et al., 2009, 2018; Zouari et al.,

2014). In addition, our analysis indicates that both mycorrhization and Pi availability triggered an organ-specific response with differential modulation of genes and apocarotenoids in roots *versus* shoots (Figs. 3 and 4).

In particular, in roots Apo9, OH-Apo9, Apo10 and OH-Apo10 are much more abundant in the MYC samples across almost all the time points analyzed and do not accumulate under +Pi, suggesting that they may be important metabolites for the AM colonization process. β-ionone, is a C13 compound produced through non enzymatic (Ramel et al., 2012) or enzymatic oxidation catalyzed by several CCD enzymes (CCD1, CCD4, and CCD7) (Fig. S9). Several studies indicate a role of this apocarotenoid in response to biotic and abiotic stress in the epigean organs of several plant species (Wilson et al., 1981; Sharma et al., 2012; Ramel et al., 2012). However, its specific involvement in the AM symbiosis has not been reported yet. Considering the increased β-ionone content in mycorrhizal roots at 21 and 35 dpi, we evaluated the impact of an exogenous β-ionone treatment on mycorrhization. We provide here the first evidence for a promoting effect of β-ionone on AM symbiosis. Notably, β-ionone has been reported to improve plant response against herbivores, bacteria and pathogenic fungi (Griffin et al., 1999; Giuliano et al., 2003; Wei et al., 2011; Cáceres et al., 2016; Aloum et al., 2020) by modulating different defense pathways (Felemban et al., 2023). As in our dataset, CCD7 displays an AM-responsive expression profile at 21 and 35 dpi, we envisage that β-ionone accumulation in AM roots is mainly due to CCD7 activity. It is worth noting that CCD7 could also be involved in the synthesis of blumenol-type metabolites and mycorradicin, which accumulate in roots in the late stage of AM colonization (Wang et al., 2018; Fiorilli et al., 2019). Therefore, it could be hypothesized that β-ionone is a precursor of blumenols and its higher accumulation in the MYC roots is required for blumenol synthesis. However, due to lack of authentic standards, we were not able to monitor blumenol derivatives.

Interestingly, we observed the accumulation at the middle and late stages of mycorrhization of zaxinone and OH-Apo10, which is the precursor of zaxinone, indicating that mycorrhization stimulates multiple steps of this branch of the apocarotenoid biochemical pathway. Notably, the expression of *ZAS1* was also highly influenced by the MYC condition in roots, confirming its correlation with zaxinone (Figs. 1 and 5). The association between *CCD8* and *ZAS1* at 7 dpi is in line with previous data showing their interplay at the early stage of the AM symbiosis (Votta et al., 2022). Apo11 level increased at 7 dpi and decreased at 21 dpi, while OH-Apo11 and OH-Apo11 isomer could be associated with the 21 dpi MYC condition. Importantly, the apocarotenoids Apo11 and OH-Apo11 were recently described as being part of an alternative zeaxanthin epoxidase-independent pathway to produce ABA (Jia et al., 2022). Moreover, these compounds act like ABA in maintaining seed dormancy and inducing the expression of ABA-responsive genes (Zheng et al., 2021; Jia et al., 2022). In light of these findings, we could hypothesize that Apo11 and OH-Apo11 could be involved in the AM symbiosis, and deserve more investigations along the whole colonization process and in relation to what has been already described for ABA in mycorrhizal roots (López-Ráez et al., 2010; Pozo et al., 2015).

The composition of shoot apocarotenoids seems to be most influenced by the time point considered. At 7 dpi, we observed a trend to a decrease of most apocarotenoids, especially in the +Pi compared to -Pi condition. At 21 dpi, the MYC and +Pi conditions showed a similar pattern with a general increase in the level of several apocarotenoids. At 35 dpi, MYC and +Pi conditions again displayed a similar profile, but with a general decrease of several apocarotenoids content. From these observations, it can be speculated that the similarity between the MYC and the +Pi conditions could mirror the Pi nutritional status since the AM symbiosis guarantees an improved Pi mineral nutrition mimicking the high Pi condition (Zouari et al., 2014). Moreover, our data indicate that the OH-Apo11 isomer deserves more investigation as it could be considered a shoot marker of the early stage of AM colonization.

We also attempted to associate the expression of specific genes with the accumulation of specific apocarotenoids with a data fusion approach as the genes involved in the production of many apocarotenoids are largely unknown. The reliability of the approach was confirmed by the association between *ZAS1*, *ZAS2* and zaxinone and its precursor in roots and by the correlation between *CCD7* and β-ionone (Fig. 5). In this context, we can speculate that CCD1 might be also involved in the production of hydroxylated APO9 and that *CCD4a* is linked to the production of OH-Apo15 and its isomer, since they are correlated in both organs (Fig. 5). Interestingly, a fungal *CCD*, *NosACO*, mediates Apo15 (retinal) production (Scherzinger et al., 2006), indicating that CCD4, or still unidentified CCDs, are involved in Apo15 formation during the AM symbiosis. In addition, the expression of *ZAS1* in shoots is also related to the accumulation of zaxinone, suggesting a direct involvement of this enzyme in endogenous zaxinone level in shoots.

In conclusion, our data show the specific profiles of *CCD* genes and apocarotenoids across different stages of the AM symbiosis and Pi conditions. Our datasets provided novel reliable AM markers in the roots, such as β-ionone (Apo9), OH-Apo9, Apo10 and OH-Apo10 which pinpoint the stage of AM symbiosis development. We also highlighted the presence of systemic markers in the shoots such as OH-Apo11 isomer, that could indicate the establishment of the symbiosis during the early stages, and OH-Apo10 that testifies the high Pi level in plants.

The identification of reliable metabolite markers, especially in the epigean plant tissues, would be highly useful for monitoring plant Pi level and for AM symbiosis not only in controlled but also in field condition. In particular, for AM symbiosis research, the evaluation of the presence and the functionality of AM fungi-plant association is still laborious and time-consuming, and typically requires destructive methods which imply root harvesting and evaluation by transcript analysis or microscopy (Vierheilig et al., 2005; Parádi et al., 2010).

Our dataset also pointed out a promoting role of β-ionone in the establishment of AM symbiosis that was confirmed by suppling β-ionone on mycorrhizal plants. Moreover, this combined approach is a promising tool to further dissect this complex metabolic pathway, providing a preliminary insight and suggesting putative links between enzymatic activities and apocarotenoid production.

Funding

This work was supported by grants from the Ministry of the University and Research (MUR), Italy (Progetti di Ricerca di Rilevante Interesse Nazionale - PRIN) prot. 2022CWZNZC to VF, the Competitive Research Grant [CRG 2017] [CRG 2020] given to SA-B and LL from King Abdullah University of Science and Technology and grants from the European Union -NextGenerationEU [2021 STARS Grants@Unipd programme P-NICHE] and from the University of Padova, Italy (BIRD214519) to MG.

CRediT authorship contribution statement

Cristina Votta: Conceptualization, Formal analysis, Writing – original draft. **Jian You Wang:** Conceptualization, Formal analysis, Writing – original draft. **Nicola Cavallini:** Data curation, Writing – original draft. **Francesco Savorani:** Data curation, Supervision, Writing – review & editing. **Arianna Capparotto:** Formal analysis. **Kit Xi Liew:** Formal analysis. **Marco Giovannetti:** Data curation, Writing – original draft, Writing – review & editing, Funding acquisition. **Luisa Lanfranco:** Conceptualization, Funding acquisition, Supervision, Writing – original draft, Writing – review & editing. **Salim Al-Babili:** Conceptualization, Funding acquisition, Project administration, Supervision, Writing – original draft, Writing – review & editing. **Valentina Fiorilli:** Conceptualization, Funding acquisition, Project administration, Supervision, Writing – original draft, Writing – review & editing.

Declaration of competing interest

The authors declare the following financial interests/personal relationships which may be considered as potential competing interests:

Valentina Fiorilli reports financial support was provided by Ministry of the University and Research (MUR). Salim Al-Babili reports financial support was provided by King Abdullah University of Science and Technology. Marco Giovannetti reports financial support was provided by University of Padua. If there are other authors, they declare that they have no known competing financial interests or personal relationships that could have appeared to influence the work reported in this paper.

Data availability

Data will be made available on request.

Acknowledgements

The authors would like to thank Jorge Gomez-Ariza for sharing the drawing of fungal structures present in Figs. 1 and 3.

Appendix A. Supplementary data

Supplementary data to this article can be found online at https://doi.org/10.1016/j.plaphy.2024.108366.

References

Ablazov, A., Mi, J., Jamil, M., Jia, K.-P., Wang, J.Y., Feng, Q., Al-Babili, S., 2020. The apocarotenoid zaxinone is a positive regulator of strigolactone and abscisic acid biosynthesis in Arabidopsis roots. Front. Plant Sci. 11, 578.
Ablazov, A., Votta, C., Fiorilli, V., et al., 2023. ZAXINONE SYNTHASE 2 regulates growth and arbuscular mycorrhizal symbiosis in rice. Plant Physiol. 191, 382–399.
Ahrazem, O., Gómez-Gómez, L., Rodrigo, M.J., Avalos, J., Limón, M.C., 2016. Carotenoid cleavage oxygenases from microbes and photosynthetic organisms: features and functions. Int. J. Mol. Sci. 17, 1781.
Alder, A., Jamil, M., Marzorati, M., Bruno, M., Vermathen, M., Bigler, P., Ghisla, S., Bouwmeester, H., Beyer, P., Al-Babili, S., 2012. The path from β-carotene to carlactone, a strigolactone-like plant hormone. Science 335, 1348–1351.
Aloum, L., Alefishat, E., Adem, A., Petroianu, G., 2020. Ionone is more than a violet's fragrance: a review. Molecules 25 (24), 5822.
Auldridge, M.E., McCarty, D.R., Klee, H.J., 2006. Plant carotenoid cleavage oxygenases and their apocarotenoid products. Curr. Opin. Plant Biol. 9, 315–321.
Balzergue, C., Chabaud, M., Barker, D.G., Bécard, G., Rochange, S.F., 2013. High phosphate reduces host ability to develop arbuscular mycorrhizal symbiosis without affecting root calcium spiking responses to the fungus. Front. Plant Sci. 29 (4), 426.
Bonfante, P., Requena, N., 2011. Dating in the dark: how roots respond to fungal signals to establish arbuscular mycorrhizal symbiosis. Curr. Opin. Plant Biol. 14, 451–457.
Borràs, E., Ferré, J., Boqué, R., Mestres, M., Aceña, L., Busto, O., 2015. Data fusion methodologies for food and beverage authentication and quality assessment A review. Anal. Chim. Acta 891, 1–14.
Breuillin, F., Schramm, J., Hajirezaei, M., Ahkami, A., Favre, P., Druege, U., Hause, B., Bucher, M., Kretzschmar, T., Bossolini, E., Kuhlemeier, C., Martinoia, E., Franken, P., Scholz, U., Reinhardt, D., 2010. Phosphate systemically inhibits development of arbuscular mycorrhiza in *Petunia hybrida* and represses genes involved in mycorrhizal functioning. Plant J. 64 (6), 1002–1017.
Bro, R.K., Smilde, A., 2014. Principal component analysis. Anal. Methods 6, 2812–2831.
Brundrett, M.C., 2009. Mycorrhizal associations and other means of nutrition of vascular plants: understanding the global diversity of host plants by resolving conflicting information and developing reliable means of diagnosis. Plant Soil 320, 37–77.
Bruno, M., Beyer, P., Al-Babili, S., 2015. The potato carotenoid cleavage dioxygenase 4 catalyzes a single cleavage of β-ionone ring-containing carotenes and non-epoxidated xanthophylls. Arch. Biochem. Biophys. 572, 126–133.
Bruno, M., Koschmieder, J., Wuest, F., Schaub, P., Fehling-Kaschek, M., Timmer, J., Beyer, P., Al-Babili, S., 2016. Enzymatic study on AtCCD4 and AtCCD7 and their potential to form acyclic regulatory metabolites. J. Exp. Bot. 67, 5993–6005.
Cáceres, L.A., Lakshminarayan, S., Yeung, K.K.C., McGarvey, B.D., Hannoufa, A., Sumarah, M.W., Benitez, X., Scott, I.M., 2016. Repellent and attractive effects of α-, β-, and dihydro-β-ionone to generalist and specialist herbivores. J. Chem. Ecol. 42, 107–117.
Carbonnel, S., Gutjahr, C., 2014. Control of arbuscular mycorrhiza development by nutrient signals. Front. Plant Sci. 5.
Cazzonelli, C.I., 2011. Carotenoids in nature: insights from plants and beyond. Funct. Plant Biol. 38, 833.
Charpentier, M., Sun, J., Wen, J., Mysore, K.S., Oldroyd, G.E.D., 2014. Abscisic acid promotion of arbuscular mycorrhizal colonization requires a component of the PROTEIN PHOSPHATASE 2A complex. Plant Physiol. 166, 2077–2090.
Chen, M., Arato, M., Borghi, L., Nouri, E., Reinhardt, D., 2018. Beneficial services of arbuscular mycorrhizal fungi from ecology to application. Front. Plant Sci. 9, 1270.
Chen, G.-T.E., Wang, J.Y., Jamil, M., Braguy, J., Al-Babili, S., 2022. 9-cis-β-Apo-10'-carotenal is the precursor of strigolactones in planta. Planta 256, 88.
Das, D., Paries, M., Hobecker, K., Gigl, M., Dawid, C., Lam, H.-M., Zhang, J., Chen, M., Gutjahr, C., 2022. PHOSPHATE STARVATION RESPONSE transcription factors enable arbuscular mycorrhiza symbiosis. Nat. Commun. 13, 477.
Felemban, A., Braguy, J., Zurbriggen, M.D., Al-Babili, S., 2019. Apocarotenoids involved in plant development and stress response. Front. Plant Sci. 10, 1168.
Felemban, A., Moreno, J.C., Mi, J., Ali, S., Sham, A., AbuQamar, S.F., Al-Babili, S., 2023. The apocarotenoid β-ionone regulates the transcriptome of *Arabidopsis thaliana* and increases its resistance against *Botrytis cinerea*. Plant J. https://doi.org/10.1111/tpj.16510.
Fester, T., Schmidt, D., Lohse, S., Walter, M., Giuliano, G., Bramley, P., Fraser, P., Hause, B., Strack, D., 2002. Stimulation of carotenoid metabolism in arbuscular mycorrhizal roots. Planta 216, 148–154.
Fiorilli, V., Catoni, M., Miozzi, L., Novero, M., Accotto, G.P., Lanfranco, L., 2009. Global and cell-type gene expression profiles in tomato plants colonized by an arbuscular mycorrhizal fungus. New Phytol. 184, 975–987.
Fiorilli, V., Vallino, M., Biselli, C., Faccio, A., Bagnaresi, P., Bonfante, P., 2015. Host and non-host roots in rice: cellular and molecular approaches reveal differential responses to arbuscular mycorrhizal fungi. Front. Plant Sci. 13, 6–636.
Fiorilli, V., Vannini, C., Ortolani, F., et al., 2018. Omics approaches revealed how arbuscular mycorrhizal symbiosis enhances yield and resistance to leaf pathogen in wheat. Sci. Rep. 8, 9625.
Fiorilli, V., Wang, J.Y., Bonfante, P., Lanfranco, L., Al-Babili, S., 2019. Apocarotenoids: old and new mediators of the arbuscular mycorrhizal symbiosis. Front. Plant Sci. 10, 1186.
Floß, D.S., Hause, B., Lange, P.R., Küster, H., Strack, D., Walter, M.H., 2008. Knock-down of the MEP pathway isogene 1-deoxy-d-xylulose 5-phosphate synthase 2 inhibits formation of arbuscular mycorrhiza-induced apocarotenoids, and abolishes normal expression of mycorrhiza-specific plant marker genes. Plant J. 56, 86–100.
Floss, D.S., Levy, J.G., Levesque-Tremblay, V., Pumplin, N., Harrison, M.J., 2013. DELLA proteins regulate arbuscule formation in arbuscular mycorrhizal symbiosis. Proc. Natl. Acad. Sci. USA 110, E5025–E5034.
Floss, D.S., Schliemann, W., Schmidt, J., Strack, D., Walter, M.H., 2008. RNA interference-mediated repression of MtCCD1 in mycorrhizal roots of *Medicago truncatula* causes accumulation of C27 apocarotenoids, shedding light on the functional role of CCD1. Plant Physiol. 148, 1267–1282.
Giuliano, G., Al-Babili, S., von Lintig, J., 2003. Carotenoid oxygenases: cleave it or leave it. Trends Plant Sci. 8, 145–149.
Griffin, S.G., Wyllie, S.G., Markham, J.L., Leach, D.N., 1999. The role of structure and molecular properties of terpenoids in determining their antimicrobial activity. Flavour Fragrance J. 14, 322–332.
Güimil, S., Chang, H.-S., Zhu, T., et al., 2005. Comparative transcriptomics of rice reveals an ancient pattern of response to microbial colonization. Proc. Natl. Acad. Sci. USA 102, 8066–8070.
Gutjahr, C., 2014. Phytohormone signaling in arbuscular mycorhiza development. Curr. Opin. Plant Biol. 20, 26–34.
Gutjahr, C., Parniske, M., 2013. Cell and developmental biology of arbuscular mycorrhiza symbiosis. Annu. Rev. Cell Dev. Biol. 29, 593–617.
Haider, I., Yunmeng, Z., White, F., Li, C., Incitti, R., Alam, I., Gojobori, T., Ruyter-Spira, C., Al-Babili, S., Bouwmeester, H.J., 2023. Transcriptome analysis of the phosphate starvation response sheds light on strigolactone biosynthesis in rice. Plant J. 114, 355–370.
Hammer, O., Harper, D.A.T., Ryan, P.D., 2001. PAST: paleontological statistics software package for education and data analysis. Palaeontol. Electron. 4, 9.
Harrison, M.J., 2012. Cellular programs for arbuscular mycorrhizal symbiosis. Curr. Opin. Plant Biol. 15, 691–698.
Harrison, P.J., Bugg, T.D.H., 2014. Enzymology of the carotenoid cleavage dioxygenases: reaction mechanisms, inhibition and biochemical roles. Arch. Biochem. Biophys. 544, 105–111.
Herrera-Medina, M.J., Steinkellner, S., Vierheilig, H., Ocampo Bote, J.A., García Garrido, J.M., 2007. Abscisic acid determines arbuscule development and functionality in the tomato arbuscular mycorrhiza. New Phytol. 175, 554–564.
Hewitt, E.J., 1966. Sand and Water Culture Methods Used in the Study of Plant Nutrition. Commonwealth Agricultural Bureaux, Farnham Royal, UK.
Hill, E.M., Robinson, L.A., Abdul-Sada, A., Vanbergen, A.J., Hodge, A., Hartley, S.E., 2018. Arbuscular mycorrhizal fungi and plant chemical defence: effects of colonisation on aboveground and belowground metabolomes. J. Chem. Ecol. 44, 198–208.
Hou, X., Rivers, J., León, P., McQuinn, R.P., Pogson, B.J., 2016. Synthesis and function of apocarotenoid signals in plants. Trends Plant Sci. 21, 792–803.
Huang, F.-C., Molnár, P., Schwab, W., 2009. Cloning and functional characterization of carotenoid cleavage dioxygenase 4 genes. J. Exp. Bot. 60, 3011–3022.
Ilg, A., Beyer, P., Al-Babili, S., 2009. Characterization of the rice carotenoid cleavage dioxygenase 1 reveals a novel route for geranial biosynthesis: a novel route for geranial formation. FEBS J. 276, 736–747.
Ilg, A., Bruno, M., Beyer, P., Al-Babili, S., 2014. Tomato carotenoid cleavage dioxygenases 1A and 1B: relaxed double bond specificity leads to a plenitude of dialdehydes, mono-apocarotenoids and isoprenoid volatiles. FEBS Open Bio 4, 584–593.
Jia, K.-P., Baz, L., Al-Babili, S., 2018. From carotenoids to strigolactones. J. Exp. Bot. 69, 2189–2204.
Jia, K.-P., Mi, J., Ali, S., et al., 2022. An alternative, zeaxanthin epoxidase-independent abscisic acid biosynthetic pathway in plants. Mol. Plant 15, 151–166.

Klingner, A., Bothe, H., Wray, V., Marner, F.-J., 1995. Identification of a yellow pigment formed in maize roots upon mycorrhizal colonization. Phytochemistry 38, 53–55.
Li Vigni, M., Durante, C., Cocchi, M., 2013. Chapter 3 exploratory data analysis. In: Marini, F. (Ed.), Chemometrics in Food Chemistry. Data Handling in Science and Technology. Elsevier, pp. 55–126.
Li, F., Gong, X., Liang, Y., Peng, L., Han, X., Wen, M., 2022. Characteristics of a new carotenoid cleavage dioxygenase *NtCCD10* derived from Nicotiana tabacum. Planta 17 (5), 256, 100.
López-Ráez, J.A., Charnikhova, T., Gómez-Roldán, V., et al., 2008. Tomato strigolactones are derived from carotenoids and their biosynthesis is promoted by phosphate starvation. New Phytol. 178, 863–874.
López-Ráez, J.A., Kohlen, W., Charnikhova, T., et al., 2010. Does abscisic acid affect strigolactone biosynthesis? New Phytol. 187, 343–354.
Ma, G., Zhang, L., Matsuta, A., Matsutani, K., Yamawaki, K., Yahata, M., Wahyudi, A., Motohashi, R., Kato, M., 2013. Enzymatic Formation of β-citraurin from β-cryptoxanthin and zeaxanthin by carotenoid cleavage Dioxygenase4 in the flavedo of Citrus fruit. Plant Physiol. 163, 682–695.
MacLean, A.M., Bravo, A., Harrison, M.J., 2017. Plant signaling and metabolic pathways enabling arbuscular mycorrhizal symbiosis. Plant Cell 29, 2319–2335.
Maier, W., Hammer, K., Dammann, U., Schulz, B., Strack, D., 1997. Accumulation of sesquiterpenoid cyclohexenone derivatives induced by an arbuscular mycorrhizal fungus in members of the Poaceae. Planta 202, 36–42.
Martín-Rodríguez, J.A., Huertas, R., Ho-Plágaro, T., Ocampo, J.A., Turečková, V., Tarkowská, D., Ludwig-Müller, J., García-Garrido, J.M., 2016. Gibberellin–abscisic acid balances during arbuscular mycorrhiza formation in tomato. Front. Plant Sci. 7, 1273.
Martín-Rodríguez, J.Á., León-Morcillo, R., Vierheilig, H., Ocampo, J.A., Ludwig-Müller, J., García-Garrido, J.M., 2011. Ethylene-dependent/ethylene-independent ABA regulation of tomato plants colonized by arbuscular mycorrhiza fungi. New Phytol. 190, 193–205.
McQuinn, R.P., Giovannoni, J.J., Pogson, B.J., 2015. More than meets the eye: from carotenoid biosynthesis, to new insights into apocarotenoid signaling. Curr. Opin. Plant Biol. 27, 172–179.
Mi, J., Al-Babili, S., 2019. To color or to decolor: that is the question. Mol. Plant 12, 1173–1175.
Mi, J., Jia, K.-P., Wang, J.Y., Al-Babili, S., 2018. A rapid LC-MS method for qualitative and quantitative profiling of plant apocarotenoids. Anal. Chim. Acta 1035, 87–95.
Moise, A.R., Al-Babili, S., Wurtzel, E.T., 2014. Mechanistic aspects of carotenoid biosynthesis. Chem. Rev. 114, 164–193.
Moreno, J.C., Mi, J., Alagoz, Y., Al-Babili, S., 2021. Plant apocarotenoids: from retrograde signaling to interspecific communication. Plant J. 105, 351–375.
Müller, L.M., Harrison, M.J., 2019. Phytohormones, miRNAs, and peptide signals integrate plant phosphorus status with arbuscular mycorrhizal symbiosis. Curr. Opin. Plant Biol. 50, 132–139.
Nadal, M., Paszkowski, U., 2013. Polyphony in the rhizosphere: presymbiotic communication in arbuscular mycorrhizal symbiosis. Curr. Opin. Plant Biol. 16, 473–479.
Nambara, E., Marion-Poll, A., 2005. Abscisic acid biosynthesis and catabolism. Annu. Rev. Plant Biol. 56, 165–185.
Nisar, N., Li, L., Lu, S., Khin, N.C., Pogson, B.J., 2015. Carotenoid metabolism in plants. Mol. Plant 8, 68–82.
Parádi, I., van Tuinen, D., Morandi, D., Ochatt, S., Robert, F., Jacas, L., Dumas-Gaudot, E., 2010. Transcription of two blue copper-binding protein isogenes is highly correlated with arbuscular mycorrhizal development in Medicago truncatula. Molecular plant-microbe interactions 23, 1175–1183.
Pozo, M.J., Jung, S.C., López-Ráez, J.A., Azcón-Aguilar, C., 2010. Impact of Arbuscular Mycorrhizal Symbiosis on Plant Response to Biotic Stress: the Role of Plant Defence Mechanisms. Arbuscular Mycorrhizas: Physiology and Function, pp. 193–207.
Pozo, M.J., López-Ráez, J.A., Azcón-Aguilar, C., García-Garrido, J.M., 2015. Phytohormones as integrators of environmental signals in the regulation of mycorrhizal symbioses. New Phytol. 205, 1431–1436.
Ramel, F., Birtic, S., Ginies, C., Soubigou-Taconnat, L., Triantaphylidès, C., Havaux, M., 2012. Carotenoid oxidation products are stress signals that mediate gene responses to singlet oxygen in plants. Proc. Natl. Acad. Sci. USA 3 (14), 5535–5540, 109.
Richardson, A.E., Lynch, J.P., Ryan, P.R., et al., 2011. Plant and microbial strategies to improve the phosphorus efficiency of agriculture. Plant Soil 349, 121–156.
Rodrigo, M.J., Alquézar, B., Alós, E., Medina, V., Carmona, L., Bruno, M., Al-Babili, S., Zacarías, L., 2013. A novel carotenoid cleavage activity involved in the biosynthesis of *Citrus* fruit-specific apocarotenoid pigments. J. Exp. Bot. 64, 4461–4478.
Scannerini, S., Bonfante-Fasolo, P., 1977. Unusual plasties in an endomycorrhizal root. Can. J. Bot. 55, 2471–2474.
Scherzinger, D., Ruch, S., Kloer, D.P., Wilde, A., Al-Babili, S., 2006. Retinal is formed from apo-carotenoids in *Nostoc* sp. PCC7120: *in vitro* characterization of an apo-carotenoid oxygenase. Biochem. J. 15 (3), 361–369, 398.
Schwartz, S.H., Qin, X., Zeevaart, J.D., 2001. Characterization of a novel carotenoid cleavage dioxygenase from plants. J. Biol. Chem. 276, 25208–25211.
Sharma, V., Singh, G., Kaur, H., Saxena, A.K., Ishar, M.P.S., 2012. Synthesis of β-ionone derived chalcones as potent antimicrobial agents. Bioorg. Med. Chem. Lett 22, 6343–6346.
Shi, J., Zhao, B., Zheng, S., et al., 2021. A phosphate starvation response-centered network regulates mycorrhizal symbiosis. Cell 184, 5527–5540.
Smith, S.E., Jakobsen, I., Grønlund, M., Smith, F.A., 2011. Roles of arbuscular mycorrhizas in plant phosphorus nutrition: interactions between pathways of phosphorus uptake in arbuscular mycorrhizal roots have important implications for understanding and manipulating plant phosphorus acquisition. Plant Physiol. 156, 1050–1057.
Spatafora, J.W., Chang, Y., Benny, G.L., et al., 2016. A phylum-level phylogenetic classification of zygomycete fungi based on genome-scale data. Mycologia 108, 1028–1046.
Strack, D., Fester, T., 2006. Isoprenoid metabolism and plastid reorganization in arbuscular mycorrhizal roots. New Phytol. 172, 22–34.
Sui, X., Kiser, P.D., Lintig, J von, Palczewski, K., 2013. Structural basis of carotenoid cleavage: from bacteria to mammals. Arch. Biochem. Biophys. 539, 203–213.
Tan, B.-C., Joseph, L.M., Deng, W.-T., Liu, L., Li, Q.-B., Cline, K., McCarty, D.R., 2003. Molecular characterization of the *Arabidopsis* 9-*cis* epoxycarotenoid dioxygenase gene family. Plant J.: Cell. Mol. Biol. (Sarreguemines, Fr., Online) 35, 44–56.
Trouvelot, A., Kough, J., Gianinazzi-Pearson, V., 1986. Evaluation of VA infection levels in root systems. Research for estimation methods having a functional significance. In: Gianinazzi-Pearson, V., Gianinazzi, S. (Eds.), Physiological and Genetical Aspects of Mycorrhizae. INRAPress, France, pp. 217–221.
Vierheilig, H., Schweiger, P., Brundrett, M., 2005. An overview of methods for the detection and observation of arbuscular mycorrhizal fungi in roots. Physiol. Plantarum 125, 393–404.
Vogel, J.T., Tan, B.-C., McCarty, D.R., Klee, H.J., 2008. The carotenoid cleavage dioxygenase 1 enzyme has broad substrate specificity, cleaving multiple carotenoids at two different bond positions. J. Biol. Chem. 283, 11364–11373.
Volpe, V., Chialva, M., Mazzarella, T., Crosino, A., Capitanio, S., Costamagna, L., Kohlen, W., Genre, A., 2023. Long-lasting impact of chitooligosaccharide application on strigolactone biosynthesis and fungal accommodation promotes arbuscular mycorrhiza in *Medicago truncatula*. New Phytol. 237, 2316–2331.
Votta, C., Fiorilli, V., Haider, I., et al., 2022. Zaxinone synthase controls arbuscular mycorrhizal colonization level in rice. Plant J. 111, 1688–1700.
Walter, M.H., Fester, T., Strack, D., 2000. Arbuscular mycorrhizal fungi induce the non-mevalonate methylerythritol phosphate pathway of isoprenoid biosynthesis correlated with accumulation of the 'yellow pigment' and other apocarotenoids: mycorrhizal induction of isoprenoid biosynthesis. Plant J. 21, 571–578.
Walter, M.H., Floß, D.S., Hans, J., Fester, T., Strack, D., 2007. Apocarotenoid biosynthesis in arbuscular mycorrhizal roots: contributions from methylerythritol phosphate pathway isogenes and tools for its manipulation. Phytochemistry 68, 130–138.
Walter, M.H., Floss, D.S., Strack, D., 2010. Apocarotenoids: hormones, mycorrhizal metabolites and aroma volatiles. Planta 232, 1–17.
Wang, J.Y., Chen, G.-T.E., Jamil, M., Braguy, J., Sioud, S., Liew, K.X., Balakrishna, A., Al-Babili, S., 2022. Protocol for characterizing strigolactones released by plant roots. STAR Protocols 3, 101352.
Wang, J.Y., Haider, I., Jamil, M., et al., 2019. The apocarotenoid metabolite zaxinone regulates growth and strigolactone biosynthesis in rice. Nat. Commun. 10, 810.
Wang, J.Y., Lin, P.-Y., Al-Babili, S., 2021. On the biosynthesis and evolution of apocarotenoid plant growth regulators. Semin. Cell Dev. Biol. 109, 3–11.
Wang, B., Qiu, Y.-L., 2006. Phylogenetic distribution and evolution of mycorrhizas in land plants. Mycorrhiza 16, 299–363.
Wang, M., Schäfer, M., Li, D., Halitschke, R., Dong, C., McGale, E., Paetz, C., Song, Y., Li, S., Dong, J., Heiling, S., Groten, K., Franken, P., Bitterlich, M., Harrison, M.J., Paszkowski, U., Baldwin, I.T., 2018. Blumenols as shoot markers of root symbiosis with arbuscular mycorrhizal fungi. Elife 28 (7), e37093.
Wang, W., Shi, J., Xie, Q., Jiang, Y., Yu, N., Wang, E., 2017. Nutrient exchange and regulation in arbuscular mycorrhizal symbiosis. Mol. Plant 10, 1147–1158.
Waters, M.T., Gutjahr, C., Bennett, T., Nelson, D.C., 2017. Strigolactone *Signaling and evolution*. Annu. Rev. Plant Biol. 68, 291–322.
Wei, S., Hannoufa, A., Soroka, J., Xu, N., Li, X., Zebarjadi, A., Gruber, M., 2011. Enhanced beta-ionone emission in Arabidopsis over-expressing ccd1 reduces feeding damage in vivo by the crucifer flea beetle. Environ. Entomol. 40, 1622–1630.
Wilson, D.M., Gueldner, R.C., Mckinney, J.K., Lievsay, R.H., Evans, B.D., Hill, R.A., 1981. Effect of *β*-Ionone on *Aspergillus flavus* and *Aspergillus parasiticus* growth, sporulation, morphology and aflatoxin production. JAOCS (J. Am. Oil Chem. Soc.) 58, A959–A961.
Yoneyama, K., Kisugi, T., Xie, X., Yoneyama, K., 2013. Chemistry of Strigolactones: Why and How Do Plants Produce So Many Strigolactones? Molecular Microbial Ecology of the Rhizosphere. John Wiley & Sons, Ltd, pp. 373–379.
Yoneyama, K., Xie, X., Kusumoto, D., Sekimoto, H., Sugimoto, Y., Takeuchi, Y., Yoneyama, K., 2007. Nitrogen deficiency as well as phosphorus deficiency in sorghum promotes the production and exudation of 5-deoxystrigol, the host recognition signal for arbuscular mycorrhizal fungi and root parasites. Planta 227, 125–132.
Zheng, X., Mi, J., Balakrishna, A., Liew, K.X., Ablazov, A., Sougrat, R., Al-Babili, S., 2022. *Gardenia* carotenoid cleavage dioxygenase 4a is an efficient tool for biotechnological production of crocins in green and non-green plant tissues. Plant Biotechnol. J. 20, 2202–2216.
Zheng, X., Yang, Y., Al-Babili, S., 2021. Exploring the diversity and regulation of apocarotenoid metabolic pathways in plants. Front. Plant Sci. 12, 787049.
Zhong, Y., Pan, X., Wang, R., Xu, J., Guo, J., Yang, T., Zhao, J., Nadeem, F., Liu, X., Shan, H., Xu, Y., Li, X., 2020. *ZmCCD10a* encodes a distinct type of carotenoid cleavage dioxygenase and enhances plant tolerance to low phosphate. Plant Physiol. 184, 374–392.
Zouari, I., Salvioli, A., Chialva, M., Novero, M., Miozzi, L., Tenore, G.C., Bagnaresi, P., Bonfante, P., 2014. From root to fruit: RNA-Seq analysis shows that arbuscular mycorrhizal symbiosis may affect tomato fruit metabolism. BMC Genom. 15, 221.